Article

Chinese Science Bulletin

Geology

March 2013 Vol.58 No.7: 788–795
doi: 10.1007/s11434-012-5376-8

# Late Paleozoic magmatism in South China: Oceanic subduction or intracontinental orogeny?

YU JinHai[1,2*], LIU Qian[1], HU XiuMian[1], WANG Qin[1] & O'REILLY Suzanne Y[2]

[1] *State Key Laboratory for Mineral Deposits Research, School of Earth Sciences and Engineering, Nanjing University, Nanjing 210093, China;*
[2] *GEMOC ARC National Key Centre, Department of Earth and Planetary Sciences, Macquarie University, Sydney, N.S.W. 2109, Australia*

Received March 9, 2012; accepted May 31, 2012; published online November 14, 2012

A gneissic granite with an U-Pb age of 313±4 Ma was found in northeastern Fujian Province, South China. It is an S-type granite characterized by high $K_2O$, $Al_2O_3$ and low $SiO_2$, $Na_2O$ contents with high A/CNK ratio of 1.22 for the whole rock. Zircons with stubby morphology from the gneissic granite yield $^{206}Pb/^{238}U$ ages ranging from 326 to 301 Ma with a weighted average age of 313±4 Ma, and negative $\varepsilon_{Hf}(t)$ values from −8.35 to −1.74 with Hf model ages ($T^{C}_{DM}$) of 1.43 to 1.84 Ga. This S-type granite probably originated from late Paleoproterozoic crust in intracontinental orogeny. Integrated with previous results on paleogeographic reconstruction of South China, the nature of Paleozoic basins, Early Permian volcanism and U-Pb-Hf isotope of detrital zircons from the late Paleozoic to early Mesozoic sedimentary rocks, we suggest the occurrence of a late Paleozoic orogeny in the eastern Cathaysia Block, South China. This orogenic cycle includes Late Carboniferous (340–310 Ma) orogeny (compression) episode and Early Permian (287–270 Ma) post-orogenic or intraplate extension episode. Therefore, the late Paleozoic magmatism in the southeastern South China probably occurred during the intraplate orogeny rather than the arc-related process.

**S-type granite, zircon U-Pb age, zircon Hf isotope, late Paleozoic orogeny, South China**

**Citation:** Yu J H, Liu Q, Hu X M, et al. Late Paleozoic magmatism in South China: Oceanic subduction or intracontinental orogeny? Chin Sci Bull, 2013, 58: 788−795, doi: 10.1007/s11434-012-5376-8

The South China Block (SCB) is comprised of the Yangtze Block to the northwest and the Cathaysia Block to the southeast. The Yangtze Block is characterized by Meso-Neoarchean crystalline basement in the Kongling terrain and widespread Neoproterozoic magmatic rocks in the periphery of the block [1–8]. In the Cathaysia Block, the old basement rocks include Paleoproterozoic granites and late Neoarchean metamorphic rocks of the Badu Group [9–12], with minor Neoproterozoic magmatic rocks in the Wuyishan area [13–15]. Notably, the Cathaysia Block experienced three episodes of intense Phanerozoic granitic magmatism: early Paleozoic (Caledonian), early Mesozoic (Indosinian) and late Mesozoic (Yanshanian) [16]. Although the late Paleozoic (Hercynian) magmatism was reported previously [17–19], little attention was paid due to lack of accurate dating results. In the past few years, some Permian granitic and alkaline magmatism (287–262 Ma) and metamorphism have been identified in Hainan Island and Luoding area of Guangdong Province [20–23]. Li et al. [20] interpreted that ~265 Ma granitic magmatism in Hainan Island was induced by the subduction of the Paleo-Pacific ocean plate beneath the SCB. By contrast, Xie et al. [21] argued that ~272 Ma shoshonitic intrusive rocks in Hainan Island were generated in the early stage of a post-collisional event. They related it to the amalgamation of the SCB with the Indochina-South China Sea plate during the convergence of the late Paleozoic Pangea supercontinent. Recently, 340–280 Ma detrital zircons were found in late Paleozoic sedimentary rocks in the SCB [24,25], stimulating interest in the late Paleozoic tectonics and magmatism. However, the sedimentary provenances of detrital zircons and the nature of their host magma are very difficult to decipher. Therefore, the geological significance of these zircons remains controversial.

*Corresponding author (email: jhyu@nju.edu.cn)

This study determines a Late Carboniferous granitoid in the Wufenglou village, Zhouning County of Fujian Province, which throws light on the characteristics of the late Paleozoic magmatism in the SCB and its relationship with the late Paleozoic Pangea supercontinent.

## 1 Geological background and sample description

The coastal region of the SCB can be divided into three parts by the NE-striking Zhenghe-Dabu and Changle-Nan'ao faults (Figure 1(a)). The Caledonian fold belt is located to the west of the Zhenghe-Dabu fault, containing Precambrian basement rocks, early Paleozoic sedimentary rocks and Caledonian granites, whereas late Mesozoic granites, volcanic and sedimentary rocks are dominant to the east of the fault. The Changle-Nan'ao fault along the coastline of Fujian Province separates the Pingtan-Dongshan metamorphic belt in the east from the inland Mesozoic igneous belt [26]. However, some high-grade metamorphic rocks and Paleozoic sedimentary rocks are sparsely exposed as inliers to the east of the Zhenghe-Dabu fault. It is worthy to note that these inliers are confined to the west of the Fu'an-Nanjing fault (Figure 1(a)). Although the Fu'an-Nanjing fault have not been clearly recognized due to the extensive covering of Mesozoic volcanic rocks, geophysical data show sharp gradients of bouguer gravity and aeromagnetic anomalies along the Fu'an-Nanjing fault [27]. Thus, the Fu'an-Nanjing fault is probably an important tectonic boundary constraining the distribution of old basement.

A fresh granitic gneiss sample was collected near the Wufenglou village, Zhouning County of Fujian Province, to the east of the Zhenghe-Dabu fault (Figure 1). In the 1:250000 geological map of Fuzhou region[1)], these metamorphic rocks sporadically outcropping in the study area are classified as the late Neoproterozoic Longbeixi Formation. The outcrop covers approximately 2.3 km$^2$ around the Wufenglou village, hosted by Early Cretaceous Makeng granite. The Makeng granite intrudes into Late Jurassic to Early Cretaceous volcanic rocks (the Nanyuan Formation) and is overlaid by Early Cretaceous volcanic rocks of the Zhaixia Formation. Many exposed gneisses have suffered intense weathering.

Sample FN10-5-2 is a biotite-rich granitic gneiss with porphyroclastic texture (Figure 2), suggesting that it underwent brittle-ductile deformation. Quartz grains show static recrystallization, and the elongated contours of their fine-grained aggregates indicate ductile-shear deformation. Biotite grains are also fine-grained, and K-feldspar and minor plagioclase grains show brittle cracking (Figure 2(b)). Major element contents were analyzed using an ARL 9800XP+ X-ray fluorescence spectrometer (XRF) at the Centre of Modern Analysis, Nanjing University. Sample FN10-5-2 contains $SiO_2$ content of 65.49%, $TiO_2$ of 0.59%, $Al_2O_3$ of 16.20%, total $Fe_2O_3$ of 4.17%, MnO of 0.06%,

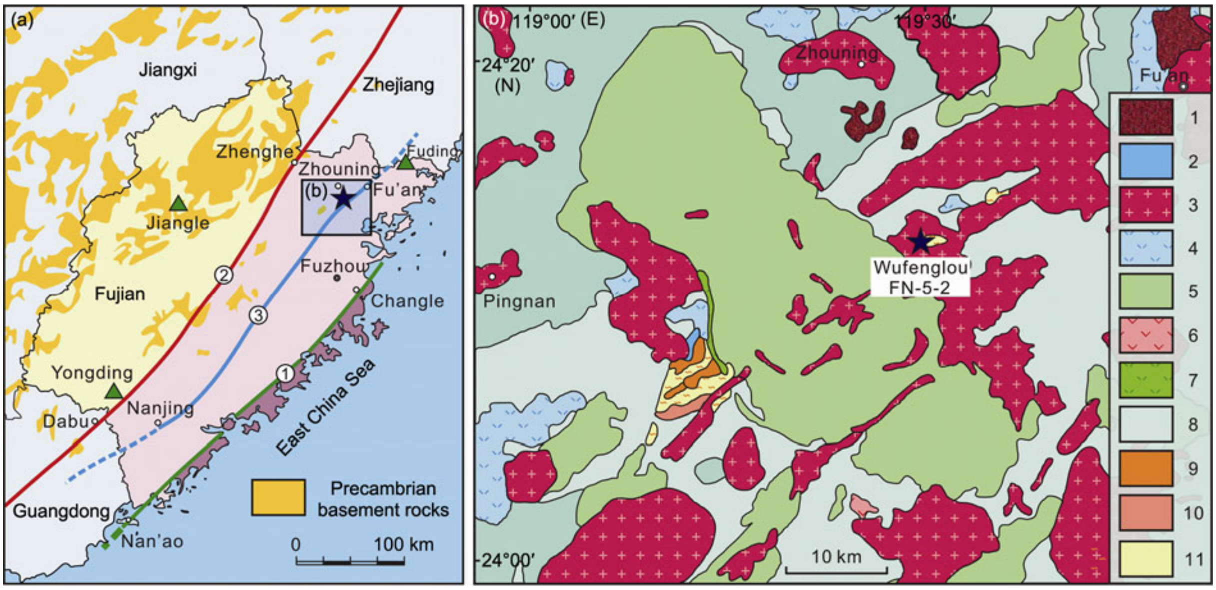


**Figure 1** (a) Geological frame of Fujian Province, eastern South China. (b) Simplified geological map of the study area (modified from 1:250000 geological map of Fuzhou region[1)]). ① the Changle-Nan'ao fault; ② the Zhenghe-Dabu fault; ③ the Fu'an-Nanjing fault. The outcrops of Precambrian strata are mainly after refs. [26]; 1, late Cretaceous intrusive rocks; 2, early Cretaceous basaltic rocks; 3, early Cretaceous granites; 4, Cretaceous subvolcanics; 5, Cretaceous sediments; 6, late Jurassic granites; 7, Jurassic subvolcanics; 8, Jurassic sediments; 9, Permian intrusive rocks; 10, Silurian intrusive rocks; 11, Carboniferous metamorphic rocks.

1) Institute of Geology Survey of Fujian Province. 1:250000 Geological Map of Fuzhou Region. 2006.

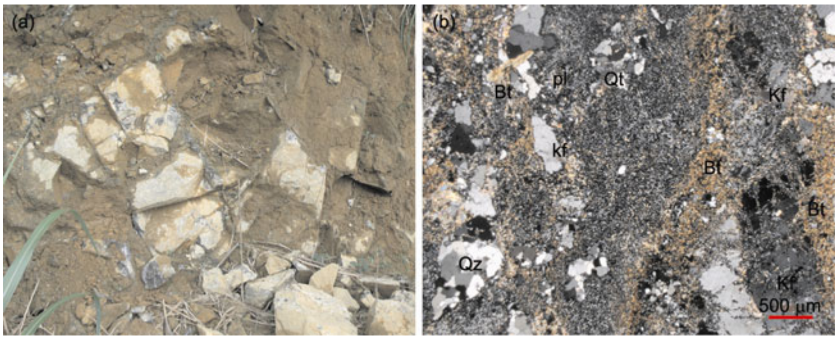


**Figure 2** Field outcrop (a) and photomicrograph (b) of the Wufenglou gneissic granite (FN10-5-2). Bt, Biotike; kf, K-feldspar; pl, plagioclase; Qz, quartz.

MgO of 1.74%, CaO of 2.07%, $Na_2O$ of 1.83%, $K_2O$ of 6.06% and $P_2O_5$ of 0.12%. Clearly, it shows an affinity with typical S-type granites characterized by high contents of $K_2O$ and $Al_2O_3$, and low $SiO_2$ and $Na_2O$ contents with low $Na_2O/K_2O$ ratio of 0.30 and high A/CNK value of 1.22.

## 2 U-Pb ages and Hf-isotope compositions of zircons

Zircon grains from the sample FN10-5-2 are prismatic to stubby prismatic, colorless to light grey, and transparent with no inclusions. They have prism faces of {110} = {100}, and pyramid faces of {101} = {211} or {101} < {211}. Most zircons display oscillatory zoning in CL images (Figure 3(a),(c)–(e)) with minor planar zoned structures (Figure 3(b)), indicating their magmatic origin. All grains do not show obvious overgrowth rims and a few have irregular inherited cores (Figure 3(d)). Th/U ratios of these zircons range from 0.13 to 0.81 with a mean of 0.34, also suggesting a magmatic genesis.

CL imaging, LA-ICPMS U-Pb dating and MC-ICPMS Hf-isotope analyses of zircons were carried out at GEMOC National Key Centre, Macquarie University, Australia. Detailed analyses procedures and corrections are referred to papers [12,28,29]. Nineteen analyzed zircons have similar ages (Table 1). Seventeen zircons with ages ranging from 326 to 301 Ma yield a weighted average $^{206}Pb/^{238}U$ age of 313±4 Ma (MSWD = 1.5) (Figure 4), which represents the intrusive age of this gneissic granite. One grain with the youngest age of 285 Ma has abnormally low Th and U contents and large analytical error, whereas the older age of 334 Ma from another grain is probably due to the minor mixing of its inherited core during laser ablation.

MC-ICPMS analyses show that thirteen zircons have relatively homogeneous Hf-isotope compositions with $^{176}Hf/^{177}Hf$ ratios of 0.282354 to 0.282534, negative $\varepsilon_{Hf}(t)$ values of −8.35 to −1.74 (a mean of −6.0) and two-stage Hf model ages ($T^{C}_{DM}$) from 1.43 Ga to 1.84 Ga (an average of 1.70 Ga) (Table 2). The results suggest that the host magma of these zircons probably derived from the late Paleoproterozoic crust [12,14].

## 3 Discussion and conclusions

Due to late metamorphism and deformation, the petrography of this granitic gneiss cannot be used directly to infer

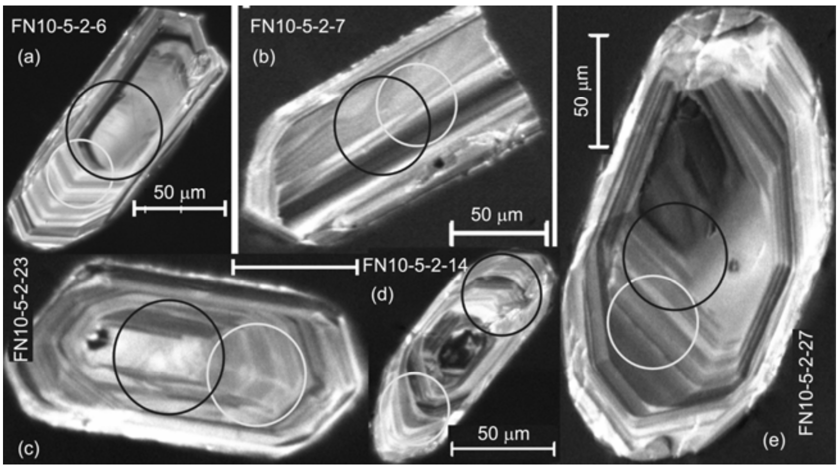


**Figure 3** CL images of zircons from the Wufenglou gneissic granite. Small circles are dating dots; big circles are Hf-isotope analysis dots; scale bars are 50 μm.

**Table 1** U-Pb ages of zircons in the Wufenglou meta-granite, Fujian Province

| Grain No. | Isotopic ratios | | | | | | Age(Ma) | | | | | | Th (ppm) | U (ppm) | Th/U |
|---|---|---|---|---|---|---|---|---|---|---|---|---|---|---|---|
| | $^{207}Pb/^{206}Pb$ | $\pm\sigma$ | $^{207}Pb/^{235}U$ | $\pm\sigma$ | $^{206}Pb/^{238}U$ | $\pm\sigma$ | $^{207}Pb/^{206}Pb$ | $\pm\sigma$ | $^{207}Pb/^{235}U$ | $\pm\sigma$ | $^{206}Pb/^{238}U$ | $\pm\sigma$ | | | |
| 1 | 0.05314 | 0.00119 | 0.36493 | 0.01272 | 0.04981 | 0.00110 | 335 | 52 | 316 | 9 | 313 | 7 | 80 | 404 | 0.20 |
| 2 | 0.05248 | 0.00107 | 0.34960 | 0.01110 | 0.04831 | 0.00101 | 306 | 48 | 304 | 8 | 304 | 6 | 311 | 404 | 0.77 |
| 2B | 0.05225 | 0.00111 | 0.34916 | 0.01140 | 0.04847 | 0.00101 | 296 | 50 | 304 | 9 | 305 | 6 | 52 | 408 | 0.13 |
| 3B | 0.05239 | 0.00160 | 0.34483 | 0.01587 | 0.04774 | 0.00119 | 302 | 71 | 301 | 12 | 301 | 7 | 81 | 407 | 0.20 |
| 4 | 0.05285 | 0.00137 | 0.35593 | 0.01392 | 0.04884 | 0.00109 | 322 | 60 | 309 | 10 | 307 | 7 | 87 | 541 | 0.16 |
| 5C | 0.05264 | 0.00196 | 0.35505 | 0.01883 | 0.04897 | 0.00115 | 313 | 87 | 309 | 14 | 308 | 7 | 85 | 361 | 0.24 |
| 6 | 0.05279 | 0.00110 | 0.34910 | 0.01090 | 0.04796 | 0.00093 | 320 | 48 | 304 | 8 | 302 | 6 | 126 | 424 | 0.30 |
| 7 | 0.05272 | 0.00108 | 0.36500 | 0.01134 | 0.05021 | 0.00100 | 317 | 48 | 316 | 8 | 316 | 6 | 260 | 347 | 0.75 |
| 8 | 0.05583 | 0.00118 | 0.38857 | 0.01271 | 0.05049 | 0.00108 | 446 | 48 | 333 | 9 | 318 | 7 | 147 | 352 | 0.42 |
| 9 | 0.05274 | 0.00089 | 0.36519 | 0.00968 | 0.05022 | 0.00097 | 318 | 39 | 316 | 7 | 316 | 6 | 103 | 520 | 0.20 |
| 10 | 0.05406 | 0.00096 | 0.38153 | 0.01037 | 0.05119 | 0.00097 | 374 | 41 | 328 | 8 | 322 | 6 | 223 | 777 | 0.29 |
| 11 | 0.05296 | 0.00118 | 0.37504 | 0.01294 | 0.05136 | 0.00113 | 327 | 52 | 323 | 10 | 323 | 7 | 81 | 481 | 0.17 |
| 12 | 0.05273 | 0.00107 | 0.36568 | 0.01142 | 0.05031 | 0.00102 | 317 | 47 | 316 | 8 | 316 | 6 | 95 | 676 | 0.14 |
| 14 | 0.05272 | 0.00104 | 0.35938 | 0.01101 | 0.04945 | 0.00101 | 317 | 46 | 312 | 8 | 311 | 6 | 312 | 384 | 0.81 |
| 20 | 0.05312 | 0.00108 | 0.37496 | 0.01168 | 0.05120 | 0.00103 | 334 | 47 | 323 | 9 | 322 | 6 | 108 | 457 | 0.24 |
| 23 | 0.05264 | 0.00116 | 0.35598 | 0.01204 | 0.04906 | 0.00105 | 313 | 51 | 309 | 9 | 309 | 6 | 188 | 454 | 0.41 |
| 27 | 0.05296 | 0.00134 | 0.37875 | 0.01471 | 0.05187 | 0.00122 | 327 | 59 | 326 | 11 | 326 | 7 | 316 | 814 | 0.39 |
| 22 | 0.05329 | 0.00116 | 0.39109 | 0.01304 | 0.05324 | 0.00111 | 341 | 50 | 335 | 10 | 334 | 7 | 75 | 395 | 0.19 |
| 3 | 0.05236 | 0.00668 | 0.32644 | 0.06038 | 0.04522 | 0.00257 | 301 | 289 | 287 | 46 | 285 | 16 | 5 | 28 | 0.18 |

**Table 2** Hf-isotope compositions of zircons in the Wufenglou gneissic granite

| Grain No. | $^{176}Hf/^{177}Hf$ | $1\sigma$ | $^{176}Lu/^{177}Hf$ | $1\sigma$ | $^{176}Yb/^{177}Hf$ | Age (Ma) | Hf *i* | $\varepsilon_{Hf}(t)$ | $T_{(DM)}$ (Ga) | $T^{C}_{(DM)}$ (Ga) |
|---|---|---|---|---|---|---|---|---|---|---|
| 2B | 0.282408 | 0.000010 | 0.00174 | 0.00002 | 0.05967 | 305 | 0.282398 | −6.53 | 1.22 | 1.73 |
| 3 | 0.282397 | 0.000011 | 0.00134 | 0.00001 | 0.05033 | 285 | 0.282390 | −7.26 | 1.22 | 1.76 |
| 3B | 0.282367 | 0.000012 | 0.00193 | 0.00005 | 0.07383 | 301 | 0.282356 | −8.11 | 1.28 | 1.82 |
| 4 | 0.282354 | 0.000023 | 0.00153 | 0.00002 | 0.06641 | 307 | 0.282345 | −8.35 | 1.29 | 1.84 |
| 6 | 0.282425 | 0.000010 | 0.00161 | 0.00002 | 0.06059 | 302 | 0.282416 | −5.97 | 1.19 | 1.69 |
| 7 | 0.282534 | 0.000011 | 0.00121 | 0.00002 | 0.04627 | 316 | 0.282527 | −1.74 | 1.02 | 1.43 |
| 9 | 0.282409 | 0.000012 | 0.00151 | 0.00002 | 0.06572 | 316 | 0.282400 | −6.22 | 1.21 | 1.72 |
| 11 | 0.282431 | 0.000011 | 0.00164 | 0.00003 | 0.07008 | 323 | 0.282421 | −5.32 | 1.18 | 1.67 |
| 14 | 0.282526 | 0.000016 | 0.00166 | 0.00002 | 0.07786 | 311 | 0.282516 | −2.21 | 1.05 | 1.46 |
| 20 | 0.282423 | 0.000007 | 0.00141 | 0.00002 | 0.05684 | 322 | 0.282415 | −5.58 | 1.19 | 1.68 |
| 22 | 0.282363 | 0.000016 | 0.00144 | 0.00002 | 0.05930 | 334 | 0.282354 | −7.44 | 1.27 | 1.81 |
| 23 | 0.282382 | 0.000007 | 0.00150 | 0.00004 | 0.05682 | 309 | 0.282373 | −7.32 | 1.25 | 1.78 |
| 27 | 0.282403 | 0.000010 | 0.00173 | 0.00003 | 0.06664 | 326 | 0.282392 | −6.27 | 1.23 | 1.73 |

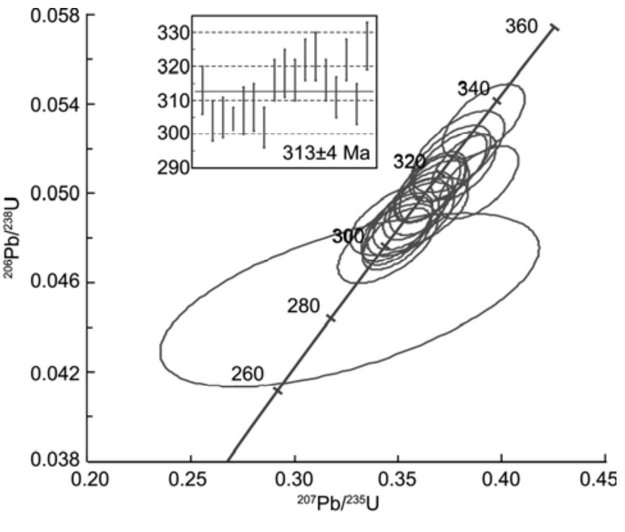


**Figure 4** U-Pb concordia diagram of zircons from the Wufenglou gneissic granite.

the protolith type, while the whole-rock composition can provide important constraint on the nature of the protolith. Generally, regional metamorphism is a closed system and makes negligible changes to major element compositions. Strong mylonitization, in some cases, may increase $SiO_2$ content and decrease contents of other oxides. In this study, the Wufenglou gneiss shows low $SiO_2$ content of 65.49% (relative to average value of granites) and weak ductile deformation, suggesting that its chemical compositions were not significantly changed. Consequently, its whole-rock composition can reflect its original components. High $K_2O$, $Al_2O_3$ contents (A/CNK = 1.22) indicate that the protolith of the Wufenglou gneiss presumably is S-type granite or sedimentary rocks (e.g. arkosic sandstone). However, euhedral morphology and same ages of zircons indicate that the protolith of this sample probably is S-type granite. Thus, the zircon U-Pb age of 313±4 Ma represents the formation age of the Wufenglou gneissic granite. It is the first report about the Late Carboniferous granitic magmatism in South China with accurate isotope chronology. Negative $\varepsilon_{Hf}(t)$ values of zircons with Hf model age of ~1.7 Ga suggest that the original magma of the S-type granite probably derived from a crust which is mainly composed of late Paleoproterozoic component. In fact, Hu et al. [24] and Li et al. [25] have reported the possible occurrence of 340–280 Ma magmatism in South China according to U-Pb ages of detrital zircons in sedimentary rocks. However, the nature and the location of host magma producing those detrital zircons have not been well constrained.

Hu et al. [24] found numerous late Paleozoic detrital zircons from Permian and Jurassic sedimentary rocks in the Fuding inlier, 90 km northeast of the Wufenglou village. The detrital zircons from their Permian sedimentary rocks exhibit an U-Pb age peak of 320–290 Ma, with minor mid-late Paleoproterozoic (1.9–1.7 Ga) and late Archean to early Paleoproterozoic (2.55–2.35 Ga) ages. The detrital zircons in the Jurassic sedimentary rocks were mainly formed at 1.85–1.75 Ga and 345–330 Ma (Figure 5). Hu et al. [24] proposed that the detrital zircons probably originated from the northeastern Cathaysia Block and recorded the late Paleozoic magmatism in the continental rifting setting. However, the lack of direct geochemical and isotope evidence of protolith hampers them to exclude an alternative scenario that the late Paleozoic magmatism occurred in the continental arc environment related to the oceanic subduction. Recently, Li et al. [25] determined late Paleozoic (~280 Ma) and early Paleozoic (~370 Ma) detrital zircons from Permian sedimentary rocks in Shaoguan, Leiyang, Ji'an and Yongding areas in the SCB (Figure 5). They attributed the ~280 Ma magmatism as an Early Permian active continental margin in southeastern China due to subduction of the Paleo-Pacific plate. However, it is well established that both oceanic arc and continental arc are characterized by the relative depletion of high field strength elements (HFSE) [30]. Consequently, element Zr is undersaturated in primary arc-type melts and thus zircon is not able to crystallize from them [30]. Thus, detrital zircons with the U-Pb age of late Paleozoic would not come from the primary arc magmas, but derive from secondary arc-derived magmas due to remelting of arc-type rocks in which Zr becomes saturated to crystallize zircon [31].

Late Paleozoic detrital zircons from the Fuding Permian sedimentary rocks in Fujian Province have negative $\varepsilon_{Hf}(t)$ values (−19.9 to −3.1, Figure 6), suggesting that these zircons probably came from S-type granitic rocks. It is consistent with the discovery of the Wufenglou gneissic S-type granite. S-type granites are generally considered to be generated in the intraplate orogeny and continental collisional orogeny [32–39]. Hence, the identification of Late Carboniferous S-type granite, coupled with the absence of coeval basaltic and andesitic magmatism in the SCB, can primarily exclude that the late Paleozoic magmatism took place in the subduction-related arc setting.

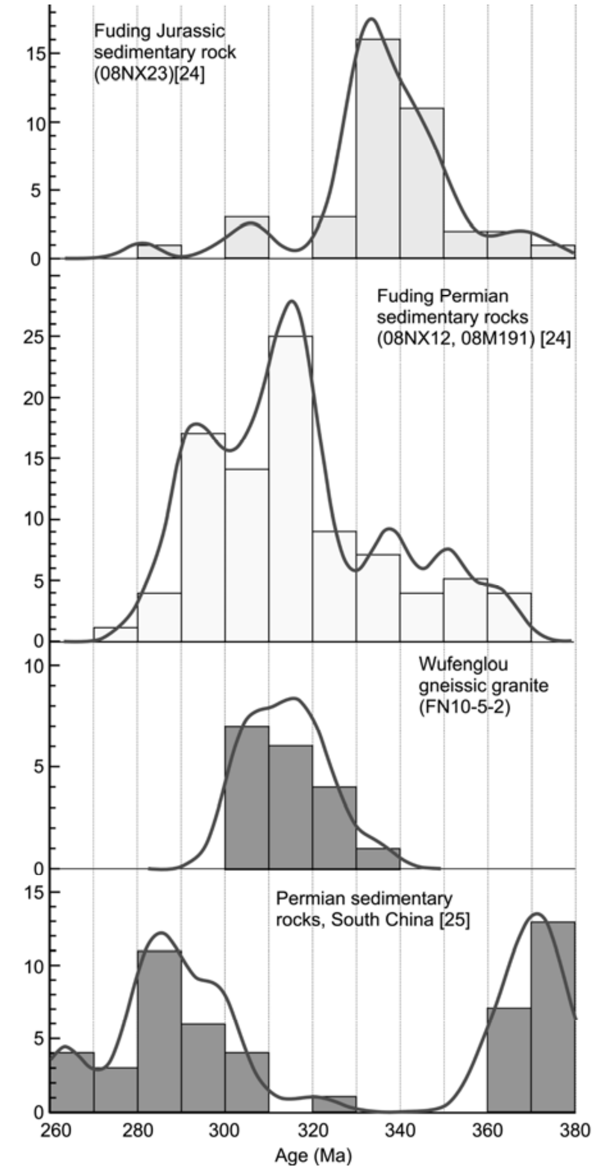


**Figure 5** Age comparison of the late Paleozoic zircons in the SCB.

In fact, the early Paleozoic (Caledonian) and the early Mesozoic (Indosinian) magmatism are also characterized by predominant S-type granites with little volcanism, sharing typical tectonic characteristics of intraplate orogeny and continental collisional orogeny [40–44]. Early Permian (~280 Ma) detrital zircons reported by Li et al. [25] have younger ages, and positive $\varepsilon_{Hf}(t)$ values (Figure 6), distinguishable from the magmatic zircons of the Wufenglou granite and the Fuding detrital zircons [24]. Therefore, Early Permian magmatism probably involves the input of juvenile materials, which is different from Late Carboniferous magmatism.

Volcanic rock interbeds in Permian sedimentary rocks were found in many places of the SCB [45–49]. Permian basaltic volcanic rocks, including pillow basalts and spilite,

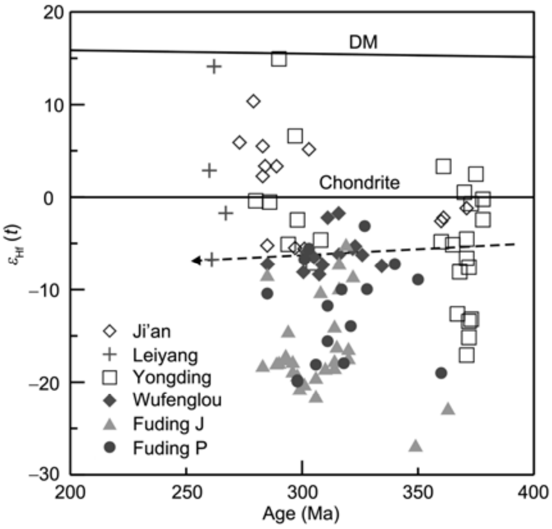


**Figure 6** Hf-isotope compositions of zircons from the Wufenglou gneissic granite. Other data source: Fuding from [24]; Ji'an, Leiyang and Yongding from [25].

were found in the western Cathaysia Block [50]. In addition, alkaline rocks with ages of 287–272 Ma were discovered in Hainan Island [21], coincident with detrital zircons reported by Li et al. [25]. These rocks were mainly generated in the extensional tectonic setting. Furthermore, Permian sedimentary basins in the SCB are intracontinental fault basins or rifting basins [51–53]. Paleogeographic reconstruction shows that the coastal region of Zhejiang-Fujian Province was an "old land" during Late Devonian to Late Carboniferous, and the entire SCB was covered by seawater in Early Permian [54–56]. Because Early Permian is regarded as global icehouse period [57–59], extensive marine sedimentation in the SCB during this period should result from the regional subsidence of a continental margin by tectonics rather than by the increase of the global sea level. All above evidence demonstrates that the SCB was subjected to an extensional tectonic setting during the Early Permian. In the extension environment, the upwelling mantle flow would induce the partial melting of the lower crust to generate volcanism [45–49] as well as the eruption of lithospheric mantle-derived basaltic magma [50]. Hence, Early Permian magmatism in the SCB is characterized by volcanism in the extensional setting, and partial melting of the juvenile crust would produce the Zr-saturated magma [30,31], consistent with positive $\varepsilon_{\mathrm{Hf}}(t)$ values of most ~280 Ma zircons [25]. Therefore, we propose that the eastern SCB experienced a late Paleozoic orogenic cycle from Late Carboniferous (340–310 Ma) orogenic (compression) episode to Early Permian (287–270 Ma) post-orogenic or intraplate extension episode. Therefore, late Paleozoic igneous rocks were induced under intraplate orogeny rather than arc-related tectonic setting.

This late Paleozoic orogeny mainly occurred in the eastern South China. The reason that it was not recognized before can be due to voluminous late Mesozoic volcanic rocks in the eastern SCB. Another possible reason is that the orogenic belt has been severely eroded. Paleogeographic reconstruction shows the eastern South China has experienced a tectonic uplifting since the late Early Permian, which may cause the extensive erosion of the orogen and westward Paleo-waterflow [25,55,56] and provide massive clastic materials to the inland basins (e.g. Shaoguan, Leiyang, Ji'an and Yongding areas). The Wufenglou gneissic granite with a U-Pb age of ~313 Ma is the direct evidence for the existence of the late Paleozoic orogen in the eastern South China.

The late Paleozoic orogeny in the eastern SCB is coincident with the significant Hercynian magmatism in Europe and assembly-breakup orogeny of the late Paleozoic Pangea supercontinent. The distribution and nature of the late Paleozoic orogen in the eastern SCB and its relationship with the Pangea supercontinent need further study.

*Most analytical work was carried out at GEMOC, Earth and Planetary Sciences, Macquarie University, using instruments funded by DEST Systemic Infrastructure Grants, ARC LIEF, NCRIS, Industry partners and Macquarie University. We thank Su Bin, Cui Xiang and Xu Hai for their help in field work, and Dr. Norman Pearson and E.A. Belousova for assistance in lab at GEMOC National Key Centre, Macquarie University, Australia. This work was supported by the National Basic Research Program of China (2012CB416701), the National Natural Science Foundation of China (40972127) and the State Key Laboratory for Mineral Deposits Research (Nanjing University) (ZZKT-201106). This is contribution 827 from the Australia Research Council National Key Centre for Geochemical Evolution and Metallogeny of Continents (www.geomoc.mq.edu.au).*

1 Li X H. U-Pb zircon ages of granites from the southern margin of the Yangtze Block: timing of Neoproterozoic Jinning: Orogeny in SE China and implications for Rodinia assembly. Precambrian Res, 1999, 97: 43–57
2 Li Z X, Li X H, Kinny P D, et al. Geochronology of Neoproterozoic syn-rift magmatism in the Yangtze Craton, South China and correlations with other continents: Evidence for a mantle superplume that broke up Rodinia. Precambrian Res, 2003, 122: 85–109
3 Qiu Y M, Gao S, McNaughton N J, et al. First evidence of >3.2 Ga continental crust in the Yangtze Craton of South China and its implications for Archean crustal evolution and Phanerozoic tectonics. Geology, 2000, 28: 11–14
4 Wang X L, Zhou J C, Qiu J S, et al. LA-ICP-MS U-Pb zircon geochronology of the Neoproterozoic igneous rocks from Northern Guangxi, South China: Implications for tectonic evolution. Precambrian Res, 2006, 122: 85–109
5 Zheng Y F, Zhang S B, Zhao Z F, et al. Contrasting zircon Hf and O isotopes in the two episodes of Neoproterozoic granitoids in South China: Implications for growth and reworking of continental crust. Lithos, 2007, 96: 127–150
6 Zheng Y F, Wu R X, Wu Y B, et al. Rift melting of juvenile arc-derived crust: Geochemical evidence from Neoproterozoic volcanic and granitic rocks in the Jiangnan Orogen, South China. Precambrian Res, 2008, 163: 351–383
7 Jiao W F, Wu Y B, Yang S H, et al. The oldest basement rock in the Yangtze Craton revealed by zircon U-Pb age and Hf isotope composition. Sci China Ser D-Earth Sci, 2009, 52: 1393–1399
8 Gao S, Yang J, Zhou L, et al. Age and growth of the Archean Kongling terrain, South China, with emphasis on 3.3 Ga granitoid gneisses. Am J Sci, 2011, 311: 153–182
9 Gan X C, Li H M, Sun D Z, et al. A geochronological study on early

Proterozoic granitic rocks, southwestern Zhejiang (in Chinese). Acta Petrol Mineral, 1995, 14: 1–8
10 Yu J H, Wang L J, O'Reilly S Y, et al. A Paleoproterozoic orogeny recorded in a long-lived cratonic remnant (Wuyishan terrane), eastern Cathaysia Block, China. Precambrian Res, 2009, 174: 347–363
11 Liu R, Zhou H W, Zhang L, et al. Paleoproterozoic reworking of ancient crust in the Cathaysia Block, South China: Evidence from zircon trace elements, U-Pb and Lu-Hf isotopes. Chin Sci Bull, 2009, 54: 1543–1554
12 Yu J H, O'Reilly S Y, Zhou M F, et al. U-Pb geochronology and Hf-Nd isotopic geochemistry of the Badu Complex, Southeastern China: implications for the Precambrian crustal evolution and paleogeography of the Cathaysia Block. Precambrian Res, 2012, (in press)
13 Li W X, Li X H, Li Z X. Neoproterozoic bimodal magmatism in the Cathaysia Block of South China and its tectonic significance. Precambrian Res, 2005, 136: 51–66
14 Wan Y S, Liu D Y, Xu M H, et al. SHRIMP U-Pb zircon geochronology and geochemistry of metavolcanic and metasedimentary rocks in Northwestern Fujian, Cathaysia Block, China: Tectonic implications and the need to redefine lithostratigraphic units. Gondwana Res, 2007, 12: 166–183
15 Shu L S, Faure M, Yu J H, et al. Geochronological and geochemical features of the Cathaysia Block (South China): New evidence for the Neoproterozoic breakup of Rodinia. Precambrian Res, 2011, 187: 263–276
16 Zhou X M, Sun T, Shen W Z, et al. Petrogenesis of Mesozoic granitoids and volcanic rocks in South China: A response to tectonic evolution. Episodes, 2006, 29: 26–33
17 Yuan K R, Yang X Y, Liang J C. Primary study of Hercynian granites in South China (in Chinese). J Guiling Coll Geol, 1981, (3): 1–28
18 Xia B D, Yu J H, Fang Z, et al. The Carboniferous bimodal volcanic rocks in Hainan Island and their plate tectonic setting (in Chinese). Acta Petrol Sin, 1991, (1): 54–62
19 Min M Z, Kong L F, Zhang G W. Isotope geochemistry of the Liuchen granite, Guangxi Province (in Chinese). Geol Rev, 1995, 41: 48–51
20 Li X H, Li Z X, Li W X, et al. Initiation of the Indosinian orogeny in South China: Evidence for a Permian magmatic arc on Hainan Island. J Geol, 2006, 114: 341–353
21 Xie C F, Zhu J C, Ding S J, et al. Identification of Hercynian shoshonitic intrusive rocks in central Hainan Island and its geotectonic implications. Chin Sci Bull, 2006, 51: 2507–2519
22 Xia B, Lin Q C, Zhang Y Q. Zircon SHRMP dating of the Longtang alkaline granite at Luoding, Guangdong, and its geological implications (in Chinese). Chin J Geol, 2006, 41: 511–517
23 Yu J H, Wang L J, Wei Z Y, et al. Phanerozoic metamorphic episodes and characteristics of Cathaysia Block (in Chinese). Geol J China Univ (Earth Sci), 2007, 13: 474–483
24 Hu X M, Huang Z C, Wang J G, et al. Geology of the Fuding inlier in southeastern China: Implication for late Paleozoic Cathaysian paleogeography. Gondwana Res, 2011, 22: 507–518
25 Li X H, Li Z X, He B, et al. The Early Permian active continental margin and crustal growth of the Cathaysia Block: *In situ* U-Pb, Lu-Hf and O isotope analyses of detrital zircons. Chem Geol, 2011, (in press)
26 Bureau of Geology and Mineral Resources of Fujian Province. Regional Geology of Fujian Province (in Chinese). Beijing: Geological Publishing House, 1985
27 Ma J Q, Xu W G. Discussion on the characteristics and geological meanings of the Fu'an-Nanjing fault zone (in Chinese). Geol Fujian, 2010, 29: 67–72
28 Griffin W L, Belousova E A, Shee S R, et al. Archean crustal evolution in the northern Yilgarn Craton: U-Pb and Hf-isotope evidence from detrital zircons. Precambrian Res, 2004, 131: 231–282
29 Jackson S E, Pearson N J, Griffin W L, et al. The application of laser ablation-inductively coupled plasma-mass spectrometry to *in-situ* U-Pb zircon geochronology. Chem Geol, 2004, 211: 47–69
30 Zheng Y F, Zhao Z F, Wu Y B, et al. Zircon U-Pb age, Hf and O isotope constraints on protolith origin of ultrahigh-pressure eclogite and gneiss in the Dabie orogen. Chem Geol, 2006, 231: 135–158
31 Zheng Y F, Xia Q X, Chen R X, et al. Partial melting, fluid supercriticality and element mobility in ultrahigh-pressure metamorphic rocks during continental collision. Earth Sci Rev, 2011, 107: 342–374
32 Pearce J A. Sources and settings of granitic rocks. Episodes, 1996, 19: 120–125
33 Searle M P, Parrish R R, Hodges K V, et al. Shisha Pangma leucogranite, South Tibetan Himalaya: Field relations, geochemistry, age, origin, and emplacement. J Geol, 1997, 105: 295–317
34 Sylvester P J. Post-collisional strongly peraluminous granites. Lithos, 1998, 45: 29–44
35 Brown M. Crustal melting and granite magmatism: Key issues. Phys Chem Earth (A), 2001, 26: 201–212
36 Atherton M P, Ghani A A. Slab breakoff: A model for Caledonian, late granite syn-collisional magmatism in the orthotectonic (metamorphic) zone of Scotland and Donegal, Ireland. Lithos, 2002, 62: 65–85
37 Sheppard S, Occhipinti S A, Tyler I M. The relationship between tectonism and composition of granitoid magmas, Yarlarweelor gneiss complex, Western Australia. Lithos, 2003, 66: 133–154
38 Healy B, Collins W J, Richards S W. A hybrid origin for Lachlan S-type granites: The Murrumbidgee Batholith example. Lithos, 2004, 78: 197–216
39 Yu J H, O'Reilly S Y, Zhao L, et al. Origin and evolution of topaz-bearing granites from the Nanling Range, South China: A geochemical and Sr-Nd-Hf isotopic study. Mineral Petrol, 2007, 90: 271–300
40 Shu L S, Yu J H, Jia D, et al. Early Paleozoic orogenic belt in the eastern segment of South China (in Chinese). Geol Bull Chin, 2008, 27: 1581–1593
41 Faure M, Shu L S, Wang B, et al. Intracontinental subduction: A possible mechanism for the Early Palaeozoic Orogen of SE China. Terra Nova, 2009, 21: 360–368
42 Charvet J, Shu L S, Faure M, et al. Structural development of the Lower Paleozoic belt of South China: Genesis of an intracontinental orogen. J Asian Earth Sci, 2010, 39: 309–330
43 Wang Y J, Fan W M, Cawood P A, et al. Indosinian high-strain deformation for the Yunkaidashan tectonic belt, south China: Kinematics and $^{40}Ar/^{39}Ar$ geochronological constraints. Tectonics, 2007, 26: TC6008, 21
44 Wang Y J, Fan W M, Zhao G C, et al. Zircon U-Pb geochronology of gneissic rocks in the Yunkai massif and its implications on the Caledonian event in the South China Block. Gondwana Res, 2007, 12: 404–416
45 Yang W R, Jiang N Y. Discovery of volcanics and radiolara in Changxing Formation from Changxing, Zhejiang Province (in Chinese). J Stratigr, 1980, 4: 64–67
46 Li G Z, Chen S S. Discovery significances of pyroclastic rocks in Upper-Permian Dalong Foramation from Hushan, Nanjing (in Chinese). Geol Rev, 1983, 29: 586–587
47 Xia B D, Zhong L R, Fang Z, et al. Early Permian Gufeng argillized volcanics in the lower Yangtze region (in Chinese). Geol Rev, 1994, 40: 64–73
48 Zhang D G. Study on the Permian volcanic eventstratigraphy in Guangdong Province (in Chinese). Coal Geol Chin, 2000, 12: 5–9
49 Long W G, Tong J N, Zhu Y H, et al. Discovery of the Permian in the Danzhou-Tunchang area of Hainan Island and its geological significance (in Chinese). Geol Miner Resour S Chin, 2007, (1): 38–45
50 Zhang B Y, Zhang H Y, Zhao Z H, et al. Permian island-arc basalt in west Guangdong and east Guangxi tectonic belt, South China: Implications for the Paleotethys (in Chinese). J Nanjing Univ (Nat Sci), 2003, 39: 46–54
51 Lu Y B, Wang D, Zhou Y X, et al. Evolution of the Permian sedimentary basins in eastern China (in Chinese). Sediment Facies Palaeogeogr, 1991, (2): 22–30
52 Chen H D, Wang C S, Liu W J, et al. Permian sequence stratigraphy and basin evolution in south of China (in Chinese). Acta Sediment Sin, 1999, 17: 529–535
53 Chen H D, Hou M C, Liu W J, et al. Basin evolution and sequence stratigraphic framework of south of China during Hercynian cycle to

Indo-Chinese epoch (in Chinese). J Chengdu Univ Technol (Sci & Technol Ed), 2004, 31: 629–635
54 Wang H Z. Atlas of the Palaeogeography of China and Its Prospect (in Chinese). Beijing: Geological Publishing House, 1985
55 Liu B J, Xu X S. Atlas of Lithofacies and Paleogeography of South China (in Chinese). Beijing: Science Press, 1994
56 Feng Z Z, Yang Y Q, Bao Z D. Lithofacies palaeogeography of the Carboniferous in South China (in Chinese). J Palaeogeogr, 1999, 1: 75–76
57 Crowley T J, Baum S K. Modeling of Late Paleozoic glaciation. Geology, 1992, 20: 507–510
58 Crowley T J. Pangean climates. In: Klein G D, ed. Pangea: Paleoclimate, Tectonics and Sedimentation During Accretion, Zenith and Breakup of a Supercontinent. Geol Soc Am Spec Pap, 1994. 228: 25–40
59 Crowell J C. The ending of the late Paleozoic ice age during the Permian period. In: Scholle P A, Peryt T M, Ulmer-Scholle D S, eds. The Permian of Northern Pangea, Vol. 1: Paleogeography, Paleoclimate, Stratigraphy. Berlin-Heidelberg-New York: Springer Verlag, 1995. 62–74